

AWARD ACCOUNTS

SPSJ Mitsubishi Chemical Award Accounts

A Novel Polysaccharide/Polynucleotide Complex
and its Application to Bio-functional DNA Delivery SystemBy Shinichi MOCHIZUKI¹ and Kazuo SAKURAI^{1,2,*}

β -1,3-glucans such as schizophyllan (SPG) and curdlan can form a novel complex with polynucleotides through hydrogen bonding between the two main chain glucoses and the one nucleotide base. The complex can be used as carriers for therapeutically functional polynucleotides such as antisense DNA, siRNA and CpG ODN. Cellular uptake efficiency of the complexes was remarkably enhanced by attaching functional groups that can be recognized by cells. Recent immunology revealed that a receptor dectin-1, normally expressed on antigen presenting cells (APCs) such as macrophages and dendritic cells, can recognize β -1,3-glucans. This fact suggests that the complex can deliver the bound DNA to the APCs. The present article reviews the fundamental and structural studies of this novel complex as well as a recent result for applying its complex to DNA carriers.

KEY WORDS: β -1,3-Glucan / Polynucleotide / Complex / Dectin-1 / Antigen Presenting Cell / CpG DNA /

Schizophyllan (SPG, Figure 1) is produced by a fungi as an extracellular polysaccharide and belongs to the β -1,3-glucan family. It consists of the main chain β -(1 \rightarrow 3)-D-glucan and one β -(1 \rightarrow 6)-D-glycosyl side chain that links to the main chain at every three glucose residues.^{1,2} According to previous studies^{3–8} SPG adopt a triple helical structure in nature (see Figure 6C) and the triple helix of SPG (t-SPG) can be dissociated into single chains (s-SPG) in dimethylsulfoxide (DMSO) or basic solutions with pH > 13. When water is added to the s-SPG/DMSO solutions or the alkaline solutions are neutralized, t-SPG is regenerated from three s-SPG chains through hydrophobic and hydrogen-bonding interactions, being similar with the renaturation process of proteins.⁹ When homopolynucleotides are present in the renaturation process, s-SPG forms a complex with the polynucleotides instead of retrieving the original triple helix. The complexation not only provides scientifically interesting issues but also a new tool to deliver biologically functional polynucleotides to specific targets.

Recent studies have shown that synthetic oligonucleotides including antisense, CpG DNAs and siRNA are useful in treatment for various incurable diseases. The first generation of antisense oligonucleotides is in late phase clinical testing^{10–13} in various sites, while many groups propose the second generation with higher binding affinities, greater stability and lower toxicity as clinical candidates.^{14–16} However, there are a number of problems to overcome *in vivo*, such as rapid excretion *via* kidney, degradation in serum, uptake by phagocytes of the reticuloendothelial system, and inefficient endocytosis by target cells. In order to put these therapeutic oligonucleotides to practical use, an efficient drug carrier is seemed inevitable.^{17–19} A variety of supramolecular nano-carriers including liposomes,²⁰ cationic polymer complex²¹ and

various polymeric nanoparticles²² have been used to deliver antisense and siRNA oligonucleotides.^{12,23–28} Complexation of oligonucleotides with polycations is a common approach for intracellular delivery; this includes PEGylated polycations,²⁹ polyethyleneimine (PEI) complexes,^{30,31} cationic block copolymers³² and dendrimers.^{33–35} However, the large size and/or considerable toxicity^{36,37} of cationic lipid particles and cationic polymers may render them problematic candidates for *in vivo* utilization.

The fungi containing β -1,3-glucans have been used Chinese herbal medicine for long time³⁸ and among others SPG and lentinan³⁹ have been commercially distributed as medicines for various cancers and health food for activating gut immunity in Japan. Recent work has revealed that the immunostimulatory nature of β -glucans is related to the effector functions of leukocytes as well as inflammatory processes. Recently, dectin-1 was identified as a major receptor involved in the recognition of β -glucans.^{40,41} Dectin-1 was originally found as a dendritic cell (DC)-specific receptor and thus it was named after ‘dendritic-cell-associated C-type lectin-1’. However, it is revealed that dectin-1 is expressed by many other antigen presenting cells (APCs), including macrophages, monocytes, neutrophils and a subset of T cells.⁴² The APC binding ability of β -1,3-glucans implies that the glucans can specifically deliver the bound oligonucleotides to APCs.

We are in the middle of investigating fundamental properties of this novel polysaccharide/polynucleotide complex as well as developing a new method for DNA delivery using this complex. The present paper reviews the discovery of the complex, its characterization, and the delivery of CpG oligonucleotides to the APCs by using this complex in an *in vitro* and *in vivo* study.

¹Department of Chemistry and Biochemistry, The University of Kitakyushu, 1-1, Hibikino, Wakamatsu-ku, Kitakyushu Fukuoka 808-0135, Japan

²CREST, Japan Science and Technology Agency, 4-1-8, Honcho, Kawaguchi 332-0012, Japan

*To whom correspondence should be addressed (Tel: +81-93-695-3298, Fax: +81-93-695-3390, E-mail: sakurai@env.kitakyu-u.ac.jp).

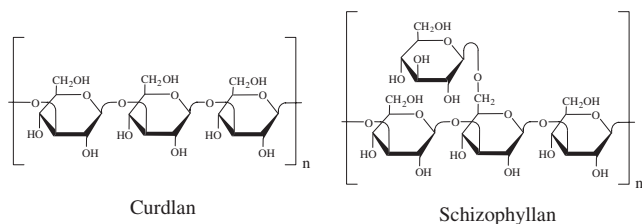


Figure 1. Chemical structures of schizophyllan (SPG) and curdlan.

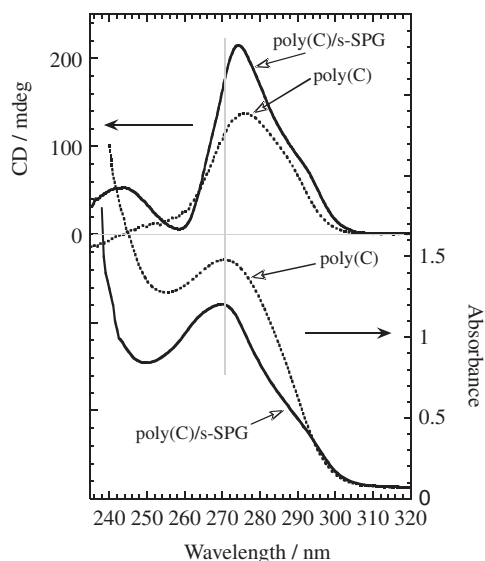


Figure 2. Comparison of the UV and CD spectra between poly(C) and poly(C) + s-SPG measured at 10 °C for a concentration of poly(C) was 7.16×10^{-3} g dL⁻¹ (2.22×10^{-4} M) with a 1 cm cell.

DISCOVERY OF COMPLEXATION BETWEEN THE β -1,3-GLUCANS AND POLYNUCLEOTIDES

SPG can form a macromolecular complex with homophosphodiester polynucleotides, such as poly(C), poly(A), poly(U), poly(T) and poly(dA), when the polynucleotide is present during the renaturation process of s-SPG.^{43–47} Figure 2 compares the ultraviolet absorbance (UV) and circular dichroism (CD) spectra between poly(C) itself and a complex made from poly(C) and s-SPG (the complex is denoted poly(C)/s-SPG).⁴⁵ Here M_w (weight average molecular weight) of s-SPG is 150 K and the cytosine base number is approximately 250. Upon the complexation, the absorbance of cytosine at 270 nm decreases by 12% (hypochromic effect) and the CD intensity of the positive peak at 275 nm increased and a new broad peak appeared at around 245 nm. Since SPG does not have absorbance within this range, the hypochromic effect of UV should be ascribed to that the stacked bases interaction was enhanced upon the complexation. Furthermore, the increment of CD intensity after the complexation implies that the polynucleotide takes an ordered helical structure, and the content of the helical structure (or an ordering of it) is increased. Consequently, the complexation creates a new

ordered helical structure of polynucleotide. This SPG-induced ordered structure is different from random aggregation induced by polycation-polynucleotide interactions, through which the CD spectrum is usually depressed.⁴⁶

Figure 3 shows the pH dependence of the CD spectra compared with poly(C) and poly(C) + s-SPG mixtures. Here, the complex forms between pH = 6.5–10 and dissociates between pH = 4–6.⁴⁸ The cytosine moiety in poly(C) becomes protonated at pH = 4–6 and dimerization of cytosine occurs with an intermolecular or intramolecular hydrogen bond. In the range pH = 6.5–10, poly(C) maintains a single stranded structure and has unoccupied hydrogen bonding sites. The pH region for the single strand is in good agreement with that of the complex, indicating that the hydrogen bonding formation between poly(C) and SPG is essential for complex formation.

Table I summarizes which homo-polynucleotide has ability to complex with SPG in natural and salt-free aqueous solutions. Poly(G), poly(U), poly(I), poly(dG) and poly(dC) show no appreciable change in their UV and CD spectra.⁴⁶ In contrast, poly(C), poly(A), poly(dA) and poly(dT) are able to form complexes with s-SPG. According to previous work, the guanines in poly(G) and poly(dG) form a tetramer or trimer.⁴⁹ In all cases, the hydrogen-bonding sites on the bases participate in intramolecular interactions. However, poly(C), poly(A), poly(dA) and poly(dT) do not form such intramolecular aggregations, thus leaving their hydrogen-bonding sites unoccupied. There is a clear correlation between complexation ability and the presence of free hydrogen-bonding sites, *i.e.*, the polynucleotide can interact with s-SPG only when hydrogen-bonding sites are available. This interaction indicates that hydrogen-bonding interactions are essential to induce the complexation.

We examined whether other polysaccharides show a similar change in UV or CD spectra when they were treated in the same manner. The results (Table II) indicate that the complexation is only observed for β -1,3-glucans. Although not shown, the natural triple helix of SPG also showed no appreciable change in its CD and UV spectra when mixed with poly(C). These indicate that the renaturation process of β -1,3-glucans is indispensable for the complexation.

Stoichiometry and Molecular Modeling of Polysaccharide/Polynucleotide Complex

To determine the stoichiometry of the complex, we examined the changes in the CD spectra of poly(C) by changing the molar ratio between polynucleotides and s-SPG. Figure 4 shows $[\theta]_{\max}$ against the molar ratio of s-SPG in the s-SPG/poly(C) mixtures, where $[\theta]_{\max}$ is the molar ellipticity at the top of the positive peak. The $[\theta]_{\max}$ value increases linearly with increasing molar ratio, following an upward convex curve, finally stabilizes at approximately 0.4. From the cross section of the plateau and increment regions, the stoichiometric ratio (N) was determined to be 0.38–0.42.⁴⁶ This result suggests that two SPG repeating units combine with three base units, namely, 8 glucoses versus 3 bases. When we examined the curdlan/poly(C) complex, the results showed 6 glucoses versus

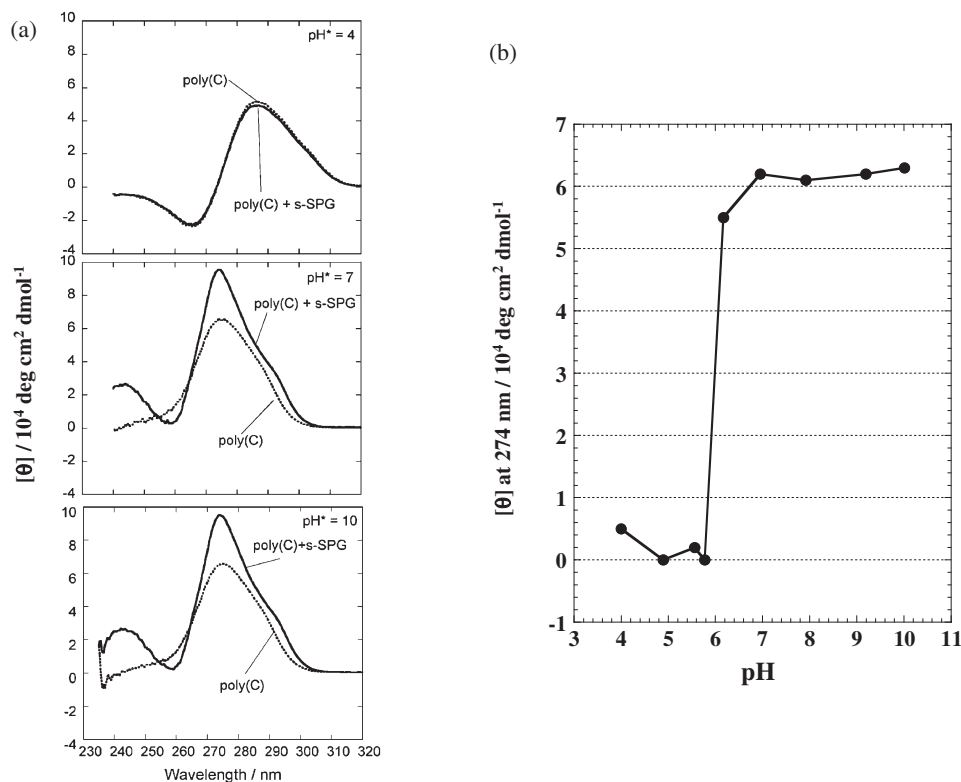


Figure 3. (a) The apparent pH dependence of the CD spectra for poly(C) (dotted lines) and its mixture with s-SPG (solid lines) measured at 10 °C. (b) pH dependence of $[\theta]_{\text{max}}$ for poly(C) itself and the poly(C)/SPG complex, where $[\theta]_{274}$ is plotted.

Table I. Nucleotide specificity in the complex formation in neutral & salt-free aqueous solution

Complex Formation		Conformation	
RNA	poly(C)	Yes	single chain
	poly(A)	Yes	single chain
	poly(U)	No	intramolecular H-bond (hairpin like)
	poly(G)	No	4G wire (intramolecular H-bond)
	poly(I)	No	intramolecular H-bond
DNA	poly(dC)	No	intramolecular H-bond
	poly(dA)	Yes	single chain
	poly(dT)	Yes	single chain
	poly(dG)	No	4G wire (intramolecular H-bond)

Table II. Relationship between the capability to form the complex and the glucose linkage of natural glucans

Name	Units	Linkage	Side chain	
Amylose	α -D-Glucose	1→4	No	No
Carrageenan	β -D-Galactose	Alternating 1→4 and 1→3	Sulfonic groups	No
Cellulose	β -D-Glucose	1→4	No	No
Dextran	α -D-Glucose	1→6	$\alpha(1\rightarrow3)$ or $\alpha(1\rightarrow4)$	No
Pullulan	α -D-Glucose	1→6	No	No
Lentinan	β -D-Glucose	1→3	$\begin{matrix} \text{G} & \text{G} \\ & \\ -\text{G}-\text{G}-\text{G}-\text{G}- \end{matrix}$	Yes
Curdlan	β -D-Glucose	1→3	$-\text{G}-\text{G}-\text{G}-\text{G}-$	Yes
Schizophyllan	β -D-Glucose	1→3	$\begin{matrix} \text{G} \\ \\ -\text{G}-\text{G}-\text{G}- \end{matrix}$	Yes

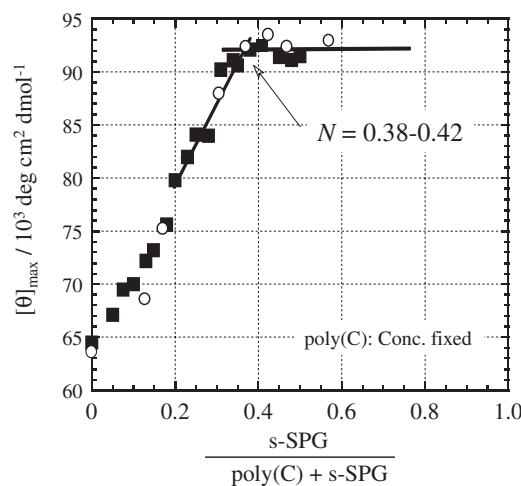


Figure 4. The job plot for the poly(C) + s-SPG system. The molar ratio is defined by $M_{\text{s-SPG}} / (M_{\text{s-SPG}} + M_{\text{poly(C)}})$, where $M_{\text{s-SPG}}$ and $M_{\text{poly(C)}}$ are the molar concentrations of poly(C) and s-SPG, respectively. The cross section of the plateau and increment regions shows that the stoichiometric ratio = 0.39–0.41. The different marks show the different series of measurements.

3 bases.⁴³ The structural difference between SPG and curdlan is the side chains; curdlan has no side chains while SPG has one glucose side chain. The discrepancy in the stoichiometric numbers can therefore be rationalized by assuming that the main chain of the β -1,3-glucans participates in the complex-

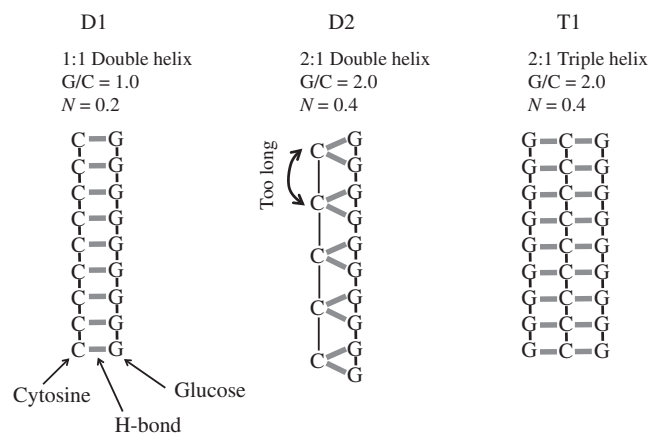


Figure 5. Three possible structures for the poly(C)/s-SPG complex. G and C denote the glucose and cytosine in the chains, respectively. In model D1, every glucose residue in the main chain interacts with the cytosine. Model T supposes that the complex adopts a triple helix similar to that existing in the β -1,3-glucans.

ation, while the side chain of SPG is not involved in the complexation.

We can postulate possible structures based on the assumptions that: (1) since the second hydroxyl groups of the main chain participate in the hydrogen-bonding interaction to stabilize the original triple-stranded helical structure of β -1,3-glucans [see Figure 6A], the same hydroxyl groups should be involved in the complex formation, (2) the side-chain glucose is not involved in complex formation (*i.e.*, the s-SPG complex is the essentially same as curdlan complex in terms of spectroscopic nature), and (3) the highly regular helical structure formed in the complex is supported by CD and UV spectral data. Figure 5 illustrates three possible structures for an s-SPG/poly(C) complex. In Model D1, every glucose residue along the main chain interacts with the cytosine residue in a DNA-like double helix. Since the distance between the neighboring main-chain glucose is about 4 Å and the stacking distance between cytosine moieties is 3.0–3.6 Å, this model would be quite reasonable stereochemically. However, the stoichiometric number ($N = 0.20$) of Model D1 does not agree

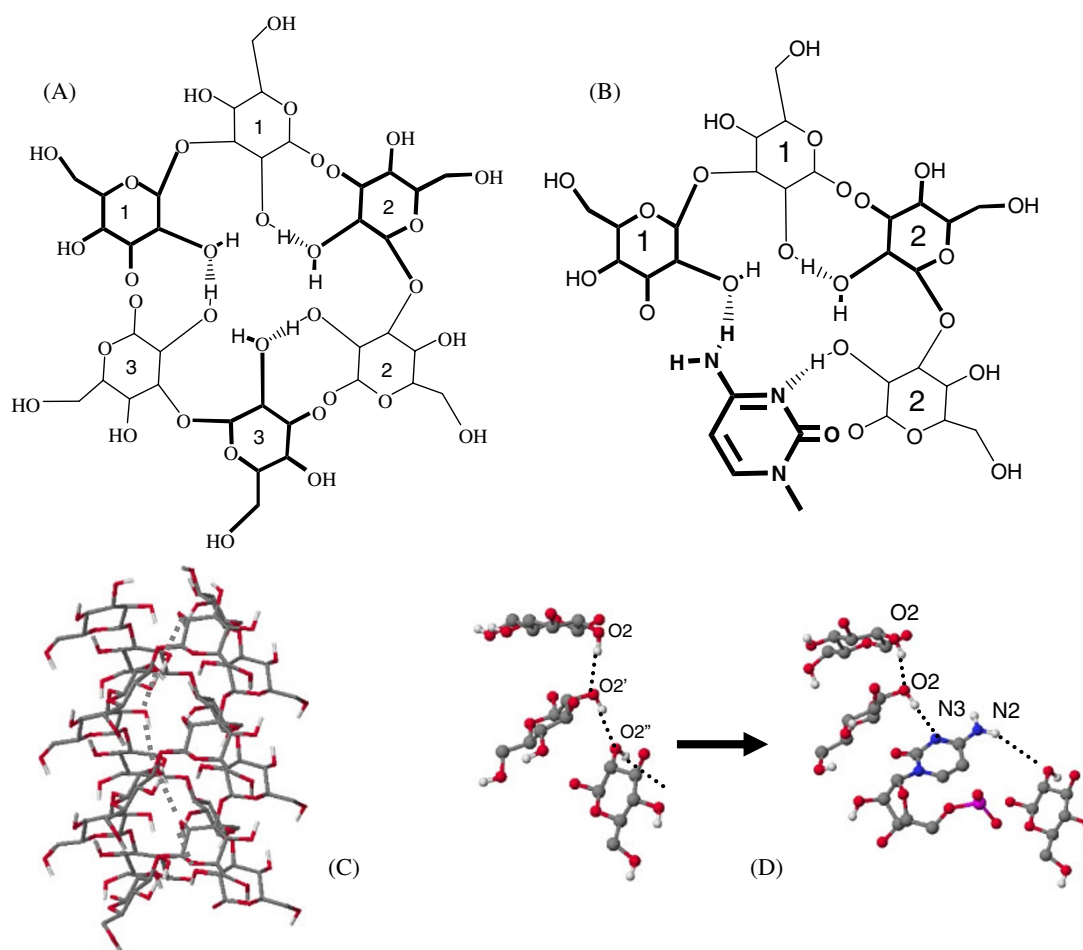


Figure 6. The left-handed helical hydrogen bond model proposed by Miyoshi *et al.*⁸² (A) a side view for the full turn triple helix, here the dot-lines indicate the hydrogen bonds and (C) a cross-sectional view of the helix (perpendicular to the helix). For convenience, only two glucoses in each chain are presented. The glucose rings marked with the same number belong to the same chain. The bold lines denote that the atoms are located at the upper position than those of the thin lines. Blue broken wedges indicate non-coplanar hydrogen bond connected along the helix, traversing three curdlan chains to make a left-handed helix. (B); Hydrogen bonds between the curdlan and the poly(C) in the complex. (D); the cross-sectional view indicates the alternation of the hydrogen bonding combination upon the complexation.

with the experimental data (Figure 4). The ribose or phosphate moieties would be stretched unfavorably (D2 in Figure 5) in order to satisfy $N = 0.40$ in the double strands which is highly unlikely. For Model T1, we supposed that complex adopted a triple-stranded helical structure similar to the original triple-stranded helical structure of SPG. When we constructed the helical structure using two s-SPG chains and one poly(C) chain, the model satisfied both the stereochemistry and the stoichiometry ($N = 0.40$) requirements. Therefore, we considered that Model T1 is the most likely structure given our experimental results.

Based on the above discussion, we constructed a structural model for the complex with computer chemistry. Firstly, we constructed the triple helix of curdlan and took one chain out of the helix. We created a poly(C) single helix referring to the crystal structure. Secondly, we tried to merge the SPG double helix and the poly(C) single helix. The poly(C) chain can fit the groove that has been created after one SPG chain is taken out because of the similarity in the helix parameters between poly(C) and SPG. Both SPG and poly(C) adopt a right-handed 6_1 helix with the similar pitch. In the third step, using the Discover 3 program and the Amber force field, we calculated the most stable conformation of poly(C) confined in the groove. The calculation was converged and indicated that poly(C) can take a conformation that is very close to the original one without creating any steric-hindrance. According to the calculated model of the complex, the cytosine can be located close to the second hydroxyl groups to form hydrogen bonding as presented in panel (Figure 6B). In the original triple helix, the intermolecular hydrogen bond array is formed as presented in Figure 6C and 6D. After complexation, one glucose is replaced by the inserted cytosine and the 3rd and 4th nitrogens in cytosine form the hydrogen bonds. Therefore, the original hydrogen bond array which had maintained the curdlan triple helix is replaced by a hybrid array which consists of the glucose *vs.* glucose hydrogen bond and the cytosine *vs.* glucose hydrogen bond as presented by the panel C.

The inset of Figure 7 shows the chromatogram of the poly(dA)₆₀/SPG complex obtained by GPC (gel permeation chromatography) coupled result multi-angle light scattering (LS) and UV. The LS intensity at 90° and the UV absorbance at $\lambda = 260$ nm show SPG and polynucleotides, respectively. Upon the complexation, the UV peak appeared at shorter elution time and the position overlapped with SPG. The radius of gyration and molecular weight were obtained from the LS data and plotted comparing with the original triple helix of SPG (t-SPG), renatured SPG (r-SPG), and batch measurements of various fractionated t-SPG samples done by Norisuye *et al.* The data points for t-SPG and the batch measurement agree with each other. The solid line was calculated from the wormlike chain model with the persistence length of 200 nm.⁷ The data of r-SPG and complex were downwardly deviated from those of t-SPG, suggesting that the conformation of r-SPG and the complex can be represented by a broken rod.

Figures 8A and 8B compares the AFM images obtained for s-SPG/poly(C) and r-SPG. For r-SPG, the image shows a

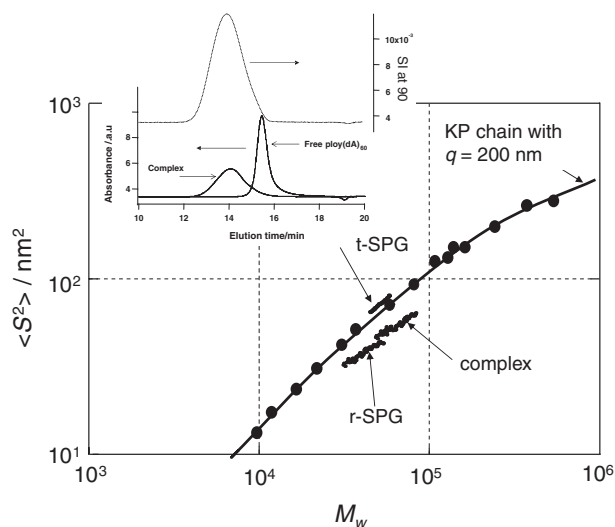


Figure 7. A typical GPC chromatogram and obtained molecular weight dependence of the radius of gyration for the native SPG (t-SPG), renatured one (r-SPG) and the complex, compared with the previously reported batch measurements by Norisuye *et al.*⁷ The solid line was calculated from the Kratky-Porod worm-like chain model with the persistence length of 200 nm.

mixture of rods and rings.⁵⁰ The image for t-SPG showed only rods with a similar length to that of the rods in panel (A). The height of each rod or ring is about 2–3 nm, being consistent with that for the schizophyllan triple helix. We measured the length of the rods (L) in this panel and plotted the results as the distribution of L in Figure 8C. The distribution seems to follow the F-distribution and has a maximum at $L_{\text{MAX}} = 180$ nm. According to Kashiwagi *et al.*,⁸ the molar mass per unit contour length (M_L) of the schizophyllan triple helix is 2170 nm^{-1} . Therefore, $L_{\text{MAX}} = 180$ nm leads to the molecular weight of 40×10^4 . This calculation indicates that the molecules with the largest population have an equivalent molecular weight to that of the original triple helix ($M_w = 45 \times 10^4$, where M_w is the weight-average molecular weight). The s-SPG/poly(C) complex showed a similar image with r-SPG while it has a different length distribution to that of r-SPG, indicating that the mixture has longer rods than r-SPG. The panel C has a second maximum at around the 300–350 nm length. Since poly(C) has 570 bases, the extended poly(C) chain is about 200 nm long and that of s-SPG is about 180 nm long. Therefore, the second maximum around 300–350 nm can appear only when more than two s-SPG chains are involved in the complexation, as illustrated in the figure.

APPLICATION OF THE COMPLEX TO AN ODN DELIVERY VEHICLE

CpG ODNs are recognized by a pattern recognition receptor called a Toll-like receptor 9 (TLR9) in endosomal compartments of APCs.^{51,52} After CpG ODN binding to TLR9, NF- κ B is induced and eventually T helper 1 (Th1) phenotype is invoked by secreting various cytokines.^{53,54} The sequence of 5'-GACGTT-3' is the key to induce an immune response from

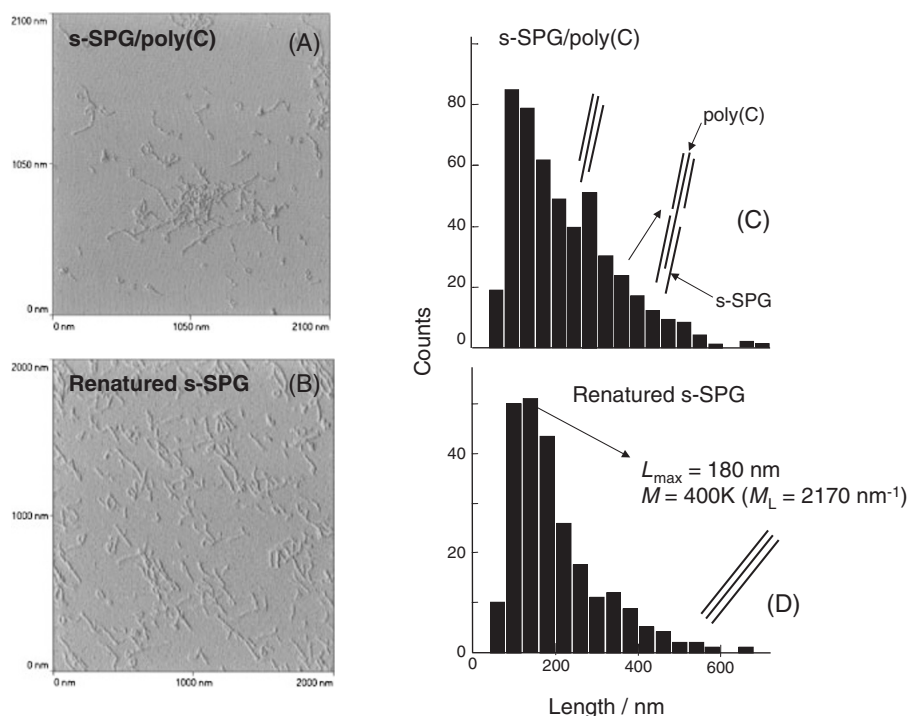


Figure 8. AFM images of the s-SPG/poly(C) complex (A) and the renatured s-SPG (B). The contour length (L) of the rod-like images in the AFM pictures was measured, using a flexible ruler (C).

murine APCs and ODNs containing this sequence are known to be excellent immune adjuvants in various murine disease models.⁵⁵ Recent studies categorized CpG ODN into at least two types of structurally and functionally different classes.^{56–59} One, denoted K-type, contains TCGT or TCGA motifs and activates plasmacytoid DCs to produce IL-6 and IL-12, but very little IFN- α or IFN- γ . K-type structures also stimulate B cells to proliferate and recreate IL-6 and IgM. The other class, D-type, contains an unmethylated CpG dinucleotide flanked by a palindromic sequence and G quartet attached to the 3'-end to increase the cellular uptake.⁶⁰ D-type structure activate plasmacytoid DCs to secrete a large amount of IFN- α , causing stimulation of NK-cells to produce IFN- γ and differentiate monocytes into myeloid dendritic cells.⁵⁸ D-type structures do not stimulate B cells and other subsets of DCs. Ballas *et al.* recently reported that D-type structure were more effective than K-type structures for the immunotherapy of murine melanoma.⁶¹

In order to use CpG ODNs therapeutically, they have to be protected from DNase mediated hydrolysis^{62,63} and be delivered to the late endosome or lysosome where TLR9 is located. Figure 9 plots v_0 against $[S]$ when the poly(C)/complex was mixed with RNaseA, comparing with naked poly(C).⁶² Here, v_0 is the initial velocity for the hydrolysis and $[S]$ is the substrate concentration. v_0 was evaluated from the initial increment in the ultraviolet absorbance (ΔAbs) at 260 nm during the hydrolysis. $[S]$ was changed from 0.07 to 0.4 mM with fixing $M_{s\text{-SPG}}/M_{\text{poly(C)}} = 1.2$ (excess of s-SPG to the stoichiometry, where $M_{s\text{-SPG}}$ and $M_{\text{poly(C)}}$ are the repeating unit molar concentrations for s-SPG and poly(C), respectively). This

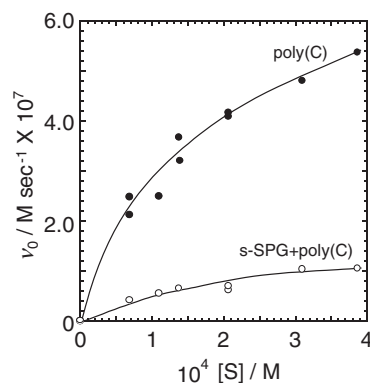


Figure 9. Increment in the ultraviolet absorbance (ΔAbs) at 260 nm during the hydrolysis of poly(C) and its complex with s-SPG. Poly(C) and its complex were hydrolyzed by RNase A in 10 mM Tris buffer (pH = 7.5) with the water/DMSO volume fraction = 0.95. The nuclease concentration was 10^{-4} g/L, and the incubation temperature was 37 °C. The increment of poly(C) fragments during the hydrolysis was measured by high-performance liquid chromatography.

figure confirms that the complexation dramatically reduces the hydrolysis rate.

In order to increase cellular-uptake for the SPG/ODN complexes without losing the complexation ability, we found a synthetic method (Figure 10) to attach a cellular-adhesive functional group to the side chain.^{64–66} In this method, the β -1,3-glucan main chain remains intact and thus able to complex with ODNs. The first step oxidizes SPG with NaIO_4 to yield formyl groups that are only generated in the side chain, because this oxidation specifically cleave 1,2-diol. The subsequent

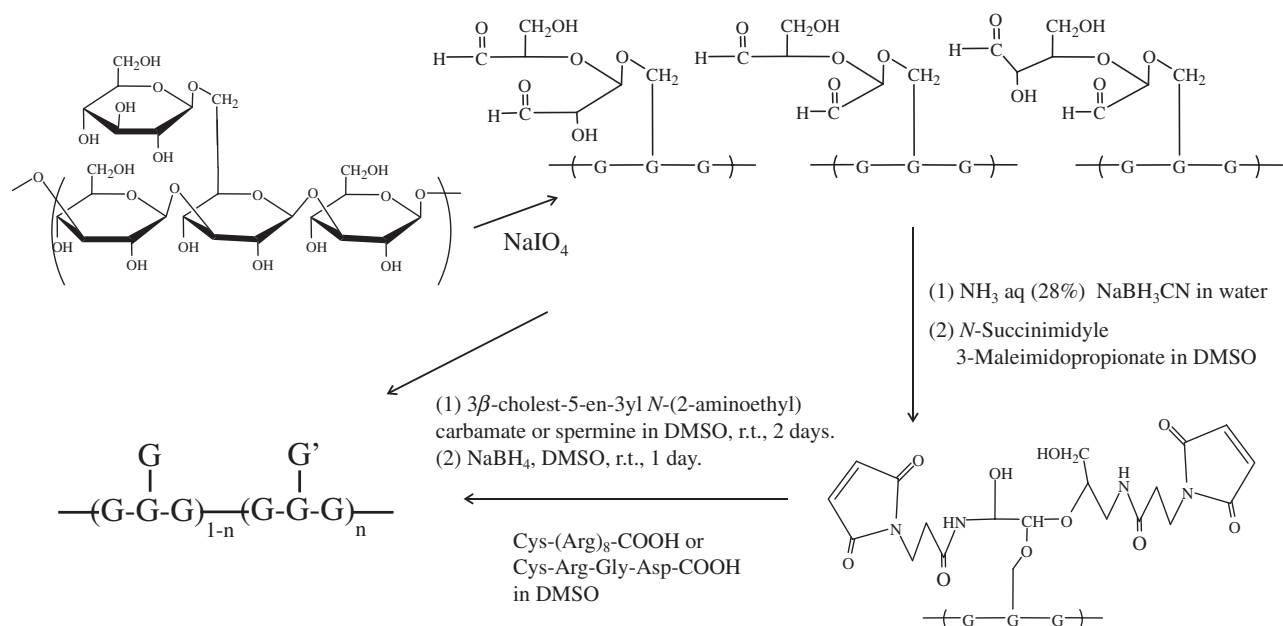


Figure 10. Schematic presentation to introduce various functional groups to the side chain of s-SPG.

Table III. Sample codes and the introduced chemical groups

Sample code	R	Modification level ^a
SP-SPG		4.6 ± 0.3 mol%
Chol-SPG		6.9 ± 1.0 mol%
R8-SPG		0.5 ± 0.1 mol%
RGD-SPG		1.3 ± 0.3 mol%

^aDetermined by N elemental analysis.

reductive amination with various cellular-adhesion groups and the formyl group can fix these functional groups to the side chains (Table III).

Figure 11 compares the cytokine secretion between the naked dose of CpG DNA and the carrier-mediated ones. When the complex of native SPG and CpG DNA (s-SPG/CpG DNA) was added, its secretion was increased by about 20–40% compared with that of the naked dose.⁶⁷ This increment can be ascribed to the SPG-mediated protection from the nuclease-mediated hydrolysis. The CpG DNA complexed with the

chemically modified SPG-derivatives increases the cytokine secretion remarkably, *i.e.*, five- to ten-fold compared with that of the naked dose. Among these SPG-derivatives, R8-SPG had the highest performance as the carrier, followed by RGD-SPG and then Chol-SPG. The difference in the performance between RGD-SPG and Chol-SPG was prominent for IL-6 but relatively small for IL-12 and TNF- α . These increases are ascribed to the increased cellular uptake mediated by the functional groups; the R8-SPG complex was the most effective, followed by the complexes of SP-SPG, and RGD-SPG, and lastly Chol-SPG.

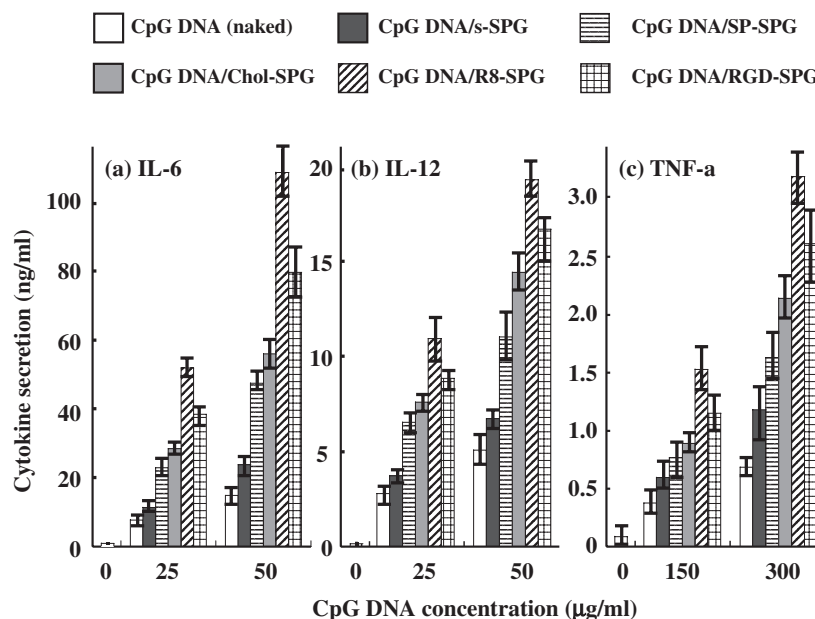


Figure 11. Effect of chemical modification of s-SPG on CpG-motif-mediated cytokine secretion. The murine macrophage-like cell J774A.1 was stimulated with various concentrations of CpG DNA for 24 h. The amount of cytokine secreted from the cells was determined by enzyme-linked immunosorbent assay. Data represent the average \pm SD ($n = 4$).

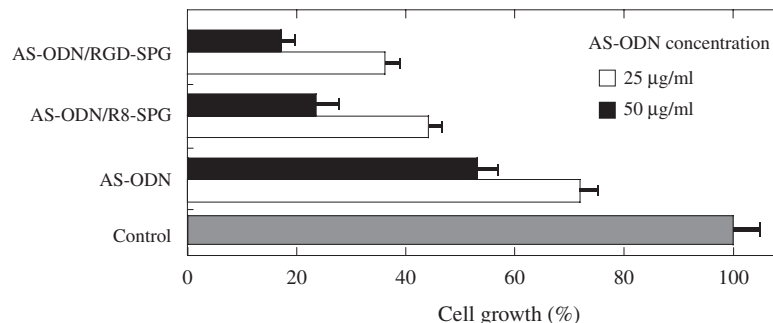


Figure 12. When A375 cells were exposed to AS-c-myb, the complexes with RGD-SPG and R8-SPG, the cell growth was measured.

According to the previous work, the cellular uptake for the SP, RGD and Chol complexes can be ascribed to normal endocytosis.^{68,69} On the other hand, the R8 complex is seemingly incorporated by an endocytosis pathway different from the other functional groups, although it is still not clear how R8 and its analogues are incorporated by cells.^{70–72} R8 binds to heparan sulfate proteoglycan which is a sulfated polysaccharide anchored to the cell surface.⁷³ The anchored heparan sulfate may release R8 and its cargo during the endocytosis transport.⁷⁴ Furthermore, Khalil *et al.* have reported that the density of R8 on the liposomes determines the uptake mechanism and that this is directly linked to intracellular trafficking, showing that a low R8 density liposomes were taken up mainly through clathrin-mediated endocytosis, whereas a high R8 density ones were taken up mainly through macropinocytosis.⁷⁵ The enhanced secretion for the R8-SPG complex may be caused by a combination of all the endocytosis pathways.

The same method can be used to carry AS ODNs.^{62–64,76,77}

Several SPG/AS ODNs complexes were prepared and then used for an antisense assay, in which phosphorotioate AS ODN was administered to melanoma A375 or leukemia HL-60 cell lines. The R8-SPG or RGD-SPG induced the strong antisense effect (Figure 12), due to the enhancement of endocytosis by the functional peptide-appendages. It should be emphasized that the tendency observed in the antisense assay is clearly consistent with that observed in the above mentioned CpG assays. These results support the view that the SPG derivatives having the cell binding appendages are potential ODNs-carriers not only protecting the therapeutic ODNs from nonselective protein absorption and enzymatic degradation but also enhancing the cellular uptake efficiency.

CpG ODN DELIVERY INTO APCs BY MEDIATING THE β -1,3-GLUCAN RECEPTOR; DECTIN-1

Dectin-1 possesses a typical C-type lectin-like carbohydrate recognition domain (CRD) and immunoreceptor tyrosine-based

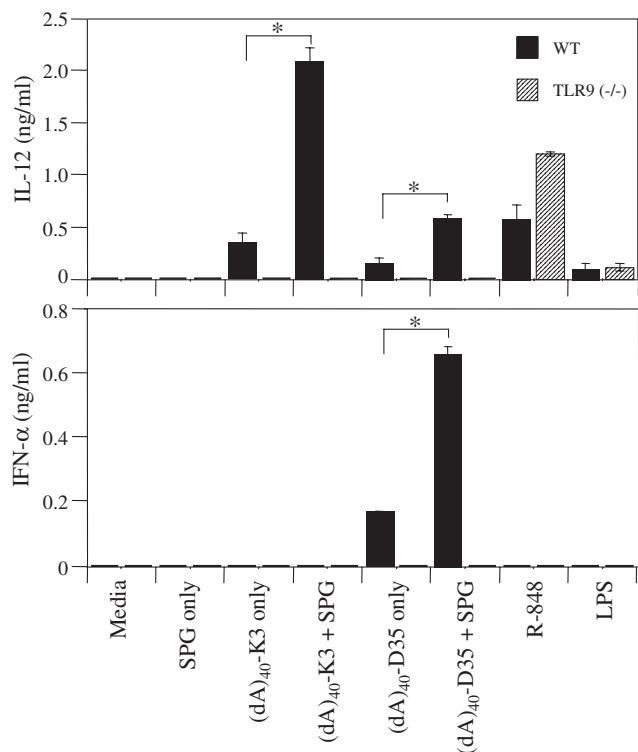


Figure 13. Difference of the cytokine secretions between K-type and D-type DNA with unmodified SPG. Flt3L ligand (Flt3L)-induced BMDCs (1×10^5 cells/well) were generated by culturing bone marrow cells with Flt3L-ligand (100 ng/ml) for 8–9 d. The cells were stimulated with CpG DNAs (30 μ g/ml), R-848 (1 μ M) or LPS (1 μ g/ml) for 24 h and the supernatants were collected for cytokine ELISA. WT and TLR9 (-/-) denote BMDCs obtained from wild type and TLR-9 knockout mice, respectively. Data represents the average \pm SD ($n = 4$), * $p < 0.01$.

activation motif (ITEM) in the cytoplasmic domain.⁷⁸ The cDNA sequence for dectin-1 indicates six cysteine residues consisting of CRD and its CRD is responsible for recognizing β -1,3-glucan moiety. The murine dectin-1 has 2 isoforms (A and B), both of which possess a CRD for binding β -glucans.⁷⁹ According to Gordon's recent work, once β -1,3-glucans are captured by dectin-1B, it seems that it is eventually ingested into the cells.⁷⁹ This fact suggests that the native-SPG/ODN complex can be used as a targeting delivery vehicle.

One distinctive difference between K- and D-type structures is in the immunological response for Flt3L-induced bone marrow-derived dendritic cells (BMDCs) which can be determined by whether the secretion of IFN- α is induced. The resultant BMDCs contain CD11c⁺/B220⁺ and CD11c⁺/B220⁻ cells.⁸⁰ K-type leads both cells to secrete IL-12; in contrast, D-type leads IFN- α secretion from CD11c⁺/B220⁺ and to IL-12 secretion from CD11c⁺/B220⁻. Therefore, when K-type is administered to the Flt3L-induced BMDCs, only IL-12 should be observed and the secretion level of IL-12 should be higher than that of D-type. In contrast, both IL-12 and IFN- α should be secreted from the D-type administration. The upper panel of Figure 13 shows the IL-12 secretion comparing (dA)₄₀-K3 and (dA)₄₀-D35, when the wild-type and TLR-9-knockout (TLR9^{-/-}) BMDCs were used. The IL-12 secretion

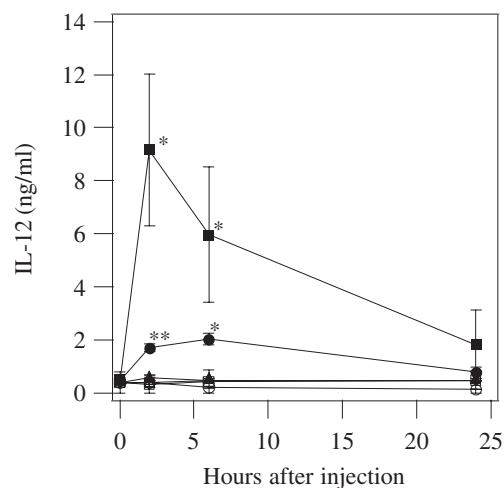


Figure 14. Time course of IL-12p40 secretion *in vivo*, when C57/BL6 mice were injected intraperitoneally with 50 μ g CpG DNAs or the complex per mouse. Serum was collected on hours. The amount of IL-12p40 in serum was determined by ELISA. Results represent the average \pm SD of three mice per group. * $p < 0.05$ when compared with naked DNAs at each time. Naked (dA)₄₀-K3 and its SPG complex are indicated with unfilled and filled squares, respectively. Naked (dA)₄₀-D35 and its complex are indicated with unfilled and filled circles, respectively. PBS alone and SPG alone are indicated with open triangles and filled triangles, respectively.

remarkably increased when (dA)₄₀-K3 was complexed. The increment due to the complexation was also observed for the case of (dA)₄₀-D35; however, the amount of the secretion was much smaller than those of (dA)₄₀-K3. These features are consistent with the difference between K- and D-type structures. The control experiment use with TLR9^{-/-} BMDCs did not secrete IL-12 at all for both (dA)₄₀-K3 and (dA)₄₀-D35 systems, while it showed a large amount of IL-12 for R848 and LPS doses, which are recognized by TLR7 and TLR4, respectively.⁸¹ These results indicate that the IL-12 production by treatment of the complex of both (dA)₄₀-K3 and (dA)₄₀-D35 can be ascribed to the signal induced by TLR9. The lower panel shows the IFN- α secretions. The K-type structure did not show any secretion; in contrast, D-type clearly showed the secretion and complexation increased the secretion levels. The present IFN- α assay clarifies the advantage of using the SPG complex for the CpG ODN delivery.

Figure 14 shows IL-12 secretion of unmodified SPG/CpG DNA complex *in vivo*.⁶⁷ IL-12 secretion was hardly observed by injection of unmodified SPG and naked CpG DNAs. On the other hand, injection of the complexes clearly exhibited 2–9 fold increase in IL-12 productions compared with those of naked doses. Maximum secretions appeared at 2–4 h. These enhancements can be ascribed to the stabilization due to the complex. Moreover, the complex with (dA)₄₀-K3 produced a large amount of IL-12 than that with (dA)₄₀-D35.

CONCLUSIONS

In this review, we have demonstrated that β -1,3-glucans have a novel feature to complex with polynucleotides,

distinguishing from other polysaccharides. The resultant complexes have well-defined helical superstructures composed of two polysaccharide-strands and one polynucleotide-strand. This unique property of β -1,3-glucans has made it possible to utilize these polysaccharide as oligo-DNA carriers. Especially, it was possible to deliver the polynucleotides into the APCs selectively without using modified SPG because of the presence of β -1,3-receptor, dectin-1, on these cells. These findings indicate that β -1,3-glucans are very attractive and useful materials in biotechnology.

Acknowledgment. K.S greatly appreciates Prof. S. Shinkai for giving him an opportunity to joint JST ICORP project in which the DMA/polysaccharide complex was found and for long collaboration after the project. K.S also thanks Dr. M. Mizu, Dr. K. Komoto, Dr. T. Anada, Dr. N. Shimada, and Dr. Y. Takeda for their enormous contribution to achieve this work. Finally and most, we thank Mitui Suger Ltd., for kindly supplying the SPG samples and finical support for long time.

Received: December 3, 2008

Accepted: January 7, 2009

Published: February 25, 2009

REFERENCES

1. K. Tabata, W. Ito, T. Kojima, S. Kawabata, and A. Misaki, *Carbohydr. Res.*, **89**, 121 (1981).
2. T. Suzuki, A. Tsuzuki, N. Ohno, Y. Ohshima, Y. Adachi, and T. Yadomae, *Biol. Pharm. Bull.*, **25**, 140 (2002).
3. E. D. T. Atkins and K. D. Parker, *Nature*, **220**, 784 (1968).
4. T. Bluhm and A. Sarko, *Can. J. Chem.*, **55**, 293 (1977).
5. Y. Deslandes, R. H. Marchessault, and A. Sarko, *Macromolecules*, **13**, 1466 (1980).
6. T. Yanaki, T. Norisuye, and H. Fujita, *Macromolecules*, **13**, 1462 (1980).
7. T. Norisuye, T. Yanaki, and H. Fujita, *J. Polym. Sci., Polym. Phys. Ed.*, **18**, 547 (1980).
8. Y. Kashiwagi, T. Norisuye, and H. Fujita, *Macromolecules*, **14**, 1220 (1981).
9. T. Sato, T. Norisuye, and H. Fujita, *Macromolecules*, **16**, 185 (1983).
10. R. Nahta and F. J. Esteva, *Semin. Oncol.*, **30**, 143 (2003).
11. N. M. Dean and C. F. Bennett, *Oncogene*, **22**, 9087 (2003).
12. J. H. Chan, S. Lim, and W. S. Wong, *Clin. Exp. Pharmacol. Physiol.*, **33**, 533 (2006).
13. F. M. Coppelli and J. R. Grandis, *Curr. Pharm. Des.*, **11**, 2825 (2005).
14. M. Manoharan, *Antisense Nucleic Acid Drug Dev.*, **12**, 103 (2002).
15. J. Kurreck, *Eur. J. Biochem.*, **270**, 1628 (2003).
16. S. T. Crooke, *Annu. Rev. Med.*, **55**, 61 (2004).
17. S. Akhtar and I. F. Benter, *J. Clin. Invest.*, **117**, 3623 (2007).
18. A. Mescalchin, A. Detzer, M. Wecke, M. Overhoff, W. Wunsche, and G. Sczakiel, *Expert Opin. Biol. Ther.*, **7**, 1531 (2007).
19. V. Russ and E. Wagner, *Pharm. Res.*, **24**, 1047 (2007).
20. D. C. Drummond, O. Meyer, K. Hong, D. B. Kirpotin, and D. Papahadjopoulos, *Pharmacol. Res.*, **51**, 691 (1999).
21. M. J. Tiera, F. O. Winnik, and J. C. Fernandes, *Curr. Gene Ther.*, **6**, 59 (2006).
22. E. M. Pridgen, R. Langer, and O. C. Farokhzad, *Nanomed*, **2**, 669 (2007).
23. A. Inoue, S. Y. Sawata, and K. Taira, *J. Drug Targeting*, **14**, 448 (2006).
24. D. De Paula, M. V. Bentley, and R. I. Mahato, *RNA*, **13**, 431 (2007).
25. I. R. Gilmore, S. P. Fox, A. J. Hollins, and S. Akhtar, *Curr. Drug Delivery*, **3**, 147 (2006).
26. W. Li and F. C. Szoka, Jr., *Pharm. Res.*, **24**, 438 (2007).
27. E. Fattal, P. Couvreur, and C. Dubernet, *Adv. Drug Delivery Rev.*, **56**, 931 (2004).
28. S. V. Vinogradov, E. V. Batrakova, and A. V. Kabanov, *Bioconjugate Chem.*, **15**, 50 (2004).
29. M. Meyer, A. Philipp, R. Oskuee, C. Schmidt, and E. Wagner, *J. Am. Chem. Soc.*, **130**, 3272 (2008).
30. M. Grzelinski, B. Urban-Klein, T. Martens, K. Lamszus, U. Bakowsky, S. Hobel, F. Czubayko, and A. Aigner, *Hum. Gene Ther.*, **17**, 751 (2006).
31. R. M. Schifflers, A. Ansari, J. Xu, Q. Zhou, Q. Tang, G. Storm, G. Molema, P. Y. Lu, P. V. Scaria, and M. C. Woodle, *Nucleic Acids Res.*, **32**, e149 (2004).
32. J. DeRouchey, C. Schmidt, G. F. Walker, C. Koch, C. Plank, E. Wagner, and J. O. Radler, *Biomacromolecules*, **9**, 724 (2008).
33. H. Kang, R. DeLong, M. H. Fisher, and R. L. Juliano, *Pharm. Res.*, **22**, 2099 (2005).
34. T. Tsutsumi, F. Hirayama, K. Uekama, and H. Arima, *J. Controlled Release*, **119**, 349 (2007).
35. H. Yoo and R. L. Juliano, *Nucleic Acids Res.*, **28**, 4225 (2000).
36. H. Lv, S. Zhang, B. Wang, S. Cui, and J. Yan, *J. Controlled Release*, **114**, 100 (2006).
37. S. Akhtar and I. Benter, *Adv. Drug Delivery Rev.*, **59**, 164 (2007).
38. C. Hobbs, "Medical Mushrooms," Botanical Press, 1991, pp 158–159.
39. G. Chihara, Y. Maeda, J. Hamuro, T. Sasaki, and F. Fukuoka, *Nature*, **222**, 687 (1969).
40. G. D. Brown and S. Gordon, *Nature*, **413**, 36 (2001).
41. G. D. Brown, P. R. Taylor, D. M. Reid, J. A. Willment, D. L. Williams, L. Martinez-Pomares, S. Y. Wong, and S. Gordon, *J. Exp. Med.*, **196**, 407 (2002).
42. P. R. Taylor, G. D. Brown, D. M. Reid, J. A. Willment, L. Martinez-Pomares, S. Gordon, and S. Y. Wong, *J. Immunol.*, **169**, 3876 (2002).
43. K. Koumoto, T. Kimura, H. Kobayashi, K. Sakurai, and S. Shinkai, *Chem. Lett.*, 908 (2001).
44. K. Miyoshi, K. Uezu, K. Sakurai, and S. Shinkai, *Chem. Biodivers.*, **1**, 916 (2004).
45. K. Sakurai and S. Shinkai, *J. Am. Chem. Soc.*, **122**, 4520 (2000).
46. K. Sakurai, M. Mizu, and S. Shinkai, *Biomacromolecules*, **2**, 641 (2001).
47. K. Koumoto, T. Kimura, M. Mizu, T. Kunitake, K. Sakurai, and S. Shinkai, *J. Chem. Soc., Perkin Trans. 1*, 2477 (2002).
48. K. Sakurai, R. Iguchi, M. Mizu, K. Koumoto, and S. Shinkai, *Bioorg. Chem.*, **31**, 216 (2003).
49. W. Saenger, "Principles of Nucleic Acid Structure," Springer-Verlag, Tokyo, 1987.
50. A. H. Bae, S. W. Lee, M. Ikeda, M. Sano, S. Shinkai, and K. Sakurai, *Carbohydr. Res.*, **339**, 251 (2004).
51. H. Henmi, O. Takeuchi, T. Kawai, T. Kaisho, S. Sato, H. Sanjo, M. Matsumoto, K. Hoshino, H. Wagner, K. Takeda, and S. Akira, *Nature*, **408**, 740 (2000).
52. E. Latz, A. Schoenemeyer, A. Visintin, K. A. Fitzgerald, B. G. Monks, C. F. Knetter, E. Lien, N. J. Nilsen, T. Espevik, and D. T. Golenbock, *Nat. Immunol.*, **5**, 190 (2004).
53. E. Latz, A. Verma, A. Visintin, M. Gong, C. M. Sirois, D. C. Klein, B. G. Monks, C. J. McKnight, M. S. Lamphier, W. P. Duprex, T. Espevik, and D. T. Golenbock, *Nat. Immunol.*, **8**, 772 (2007).
54. H. Hacker, R. M. Vabulas, O. Takeuchi, K. Hoshino, S. Akira, and H. Wagner, *J. Exp. Med.*, **192**, 595 (2000).
55. A. M. Krieg, *Annu. Rev. Immunol.*, **20**, 709 (2002).
56. K. J. Ishii, I. Gursel, M. Gursel, and D. M. Klinman, *Curr. Opin. Mol. Ther.*, **6**, 166 (2004).
57. D. Verthelyi, K. J. Ishii, M. Gursel, F. Takeshita, and D. M. Klinman, *J. Immunol.*, **166**, 2372 (2001).
58. M. Gursel, D. Verthelyi, and D. M. Klinman, *Eur. J. Immunol.*, **32**,

- 2617 (2002).
59. M. Gursel, D. Verthelyi, I. Gursel, K. J. Ishii, and D. M. Klinman, *J. Leukocyte Biol.*, **71**, 813 (2002).
 60. V. Prasad, S. Hashim, A. Mukhopadhyay, S. K. Basu, and R. P. Roy, *Antimicrob. Agents Chemother.*, **43**, 2689 (1999).
 61. Z. K. Ballas, A. M. Krieg, T. Warren, W. Rasmussen, H. L. Davis, M. Waldschmidt, and G. J. Weiner, *J. Immunol.*, **167**, 4878 (2001).
 62. M. Mizu, K. Koumoto, T. Kimura, K. Sakurai, and S. Shinkai, *Biomaterials*, **25**, 3109 (2004).
 63. M. Mizu, K. Koumoto, T. Anada, K. Sakurai, and S. Shinkai, *Biomaterials*, **25**, 3117 (2004).
 64. T. Matsumoto, M. Numata, T. Anada, M. Mizu, K. Koumoto, K. Sakurai, T. Nagasaki, and S. Shinkai, *Biochim. Biophys. Acta*, **1670**, 91 (2004).
 65. K. Koumoto, T. Kimura, M. Mizu, K. Sakurai, and S. Shinkai, *Chem. Commun.*, 1962 (2001).
 66. M. Mizu, K. Koumoto, T. Anada, T. Matsumoto, M. Numata, S. Shinkai, T. Nagasaki, and K. Sakurai, *J. Am. Chem. Soc.*, **126**, 8372 (2004).
 67. N. Shimada, K. J. Ishii, Y. Takeda, C. Coban, Y. Torii, S. Shinkai, S. Akira, and K. Sakurai, *Bioconjugate Chem.*, **18**, 1280 (2007).
 68. H. J. Heiniger, A. A. Kandutsch, and H. W. Chen, *Nature*, **263**, 515 (1976).
 69. M. Colin, R. P. Harbottle, A. Knight, M. Kornprobst, R. G. Cooper, A. D. Miller, G. Trugnan, J. Capeau, C. Coutelle, and M. C. Brahimi-Horn, *Gene Ther.*, **5**, 1488 (1998).
 70. I. Nakase, M. Niwa, T. Takeuchi, K. Sonomura, N. Kawabata, Y. Koike, M. Takehashi, S. Tanaka, K. Ueda, J. C. Simpson, A. T. Jones, Y. Sugiura, and S. Futaki, *Mol. Ther.*, **10**, 1011 (2004).
 71. A. Ferrari, V. Pellegrini, C. Arcangeli, A. Fittipaldi, M. Giacca, and F. Beltram, *Mol. Ther.*, **8**, 284 (2003).
 72. J. L. Zaro, T. E. Rajapaksa, C. T. Okamoto, and W. C. Shen, *Mol. Pharmacol.*, **3**, 181 (2006).
 73. E. Goncalves, E. Kitas, and J. Seelig, *Biochemistry*, **44**, 2692 (2005).
 74. Y. Xu and F. C. Szoka, Jr., *Biochemistry*, **35**, 5616 (1996).
 75. I. A. Khalil, K. Kogure, S. Futaki, and H. Harashima, *J. Biol. Chem.*, **281**, 3544 (2006).
 76. T. Hasegawa, T. Fujisawa, S. Haraguchi, M. Numata, R. Karinaga, T. Kimura, S. Okumura, K. Sakurai, and S. Shinkai, *Bioorg. Med. Chem. Lett.*, **15**, 327 (2005).
 77. R. Karinaga, K. Koumoto, M. Mizu, T. Anada, S. Shinkai, and K. Sakurai, *Biomaterials*, **26**, 4866 (2005).
 78. K. Ariizumi, G. L. Shen, S. Shikano, S. Xu, R. Ritter, 3rd, T. Kumamoto, D. Edelbaum, A. Morita, P. R. Bergstresser, and A. Takashima, *J. Biol. Chem.*, **275**, 20157 (2000).
 79. S. E. Heinsbroek, P. R. Taylor, M. Rosas, J. A. Willment, D. L. Williams, S. Gordon, and G. D. Brown, *J. Immunol.*, **176**, 5513 (2006).
 80. H. Hemmi, T. Kaisho, K. Takeda, and S. Akira, *J. Immunol.*, **170**, 3059 (2003).
 81. T. Ito, R. Amakawa, T. Kaisho, H. Hemmi, K. Tajima, K. Uehira, Y. Ozaki, H. Tomizawa, S. Akira, and S. Fukuhara, *J. Exp. Med.*, **195**, 1507 (2002).
 82. K. Miyoshi, K. Uezu, K. Sakurai, and S. Shinkai, *Biomacromolecules*, **6**, 1540 (2005).



Kazuo Sakurai was born in 1958 in Gifu, Japan, and after finished the master course of Osaka University, he joined Kanebo Ltd in 1984. He spent three years (1990–1993) in USA working for Prof. MacKnight in Univ. Mass, and received PhD from Osaka University in 1996. He worked for Pro. Sinkai in JST Project at Kurume from 1999–2001 and has been a professor of the University of Kitakyushu since 2001. His major research interests are polysaccharides, polysaccharide/polynucleotide complexes, gene delivery, and small-angle X-ray scattering from soft materials.



Shinichi Mochizuki was born in 1979 in Saitama, Japan, and received his PhD in 2008 from Kyushu University. He became an assistant professor at the University of Kitakyushu in 2008. His research interests are gene delivery, and biomaterials based on nucleic acids and polysaccharides.